Antigen Binding Thermodynamics and Antiproliferative Effects of Chimeric and Humanized anti-p185^{HER2} Antibody Fab Fragments

Robert F. Kelley,*,‡ Mark P. O'Connell,‡ Paul Carter,‡ Leonard Presta,‡ Charles Eigenbrot,‡ Michael Covarrubias,§ Brad Snedecor,§ James H. Bourell,∥ and David Vetterlein⊥

Departments of Protein Engineering, Cell Culture and Fermentation Research, Protein Chemistry, and Process Sciences, Genentech, Inc., 460 Point San Bruno Blvd., South San Francisco, California 94080

Received January 2, 1992

ABSTRACT: The murine monoclonal antibody 4D5 (anti-p185^{HER2}) inhibits the proliferation of human tumor cells overexpressing p185^{HER2} in vitro and has been "humanized" [Carter, P., Presta, L., Gorman, C. M., Ridgway, J. B. B., Henner, D., Wong, W.-L. T., Rowland, A. M., Kotts, C., Carver, M. E., & Shepard, H. M. (1992) *Proc. Natl. Acad. Sci. U.S.A* (in press)] for use in human cancer therapy. We have determined the antigen binding thermodynamics and the antiproliferative activities of chimeric 4D5 Fab (ch4D5 Fab) fragment and a series of eight humanized Fab (hu4D5 Fab) fragments differing by amino acid substitutions in the framework regions of the variable domains. Fab fragments were expressed by secretion from *Escherichia coli* and purified from fermentation supernatants by using affinity chromatography on immobilized streptococcal protein G or staphylococcal protein A for ch4D5 and hu4D5, respectively. Circular dichroism spectroscopy indicates correct folding of the *E. coli* produced Fab, and scanning calorimetry shows a greater stability for hu4D5 (T_m = 82 °C) as compared with ch4D5 Fab (T_m = 72 °C). K_D values for binding to the extracellular domain (ECD) of p185^{HER2} were determined by using a radioimmunoassay; the ΔH and ΔC_p for binding were determined by using isothermal titration calorimetry. ch4D5 Fab and one of the humanized variants (hu4D5-8 Fab) bind p185$^{HER2\text{-}ECD}$ with comparable affinity ($\Delta G°$ = −13.6 kcal mol^{-1}). The enthalpy changes associated with binding, however, are considerably different (ch4D5 Fab ΔH = −17.2 ± 1.5 kcal mol^{-1}; hu4D5-8 Fab ΔH = −12.9 ± 0.4 kcal mol^{-1}), which suggests a significant difference in the mechanism of antigen binding. This difference may be important for antiproliferative activity since ch4D5 Fab retains activity whereas hu4D5-8 Fab is inactive. These results suggest that K_D measurements alone are insufficient in an attempt to reproduce the activity of a murine antibody in a humanized form. Analysis of the thermodynamic data using an empirical method [Sturtevant, J. M. (1977) *Proc. Natl. Acad. Sci. U.S.A. 74*, 2236–2240] indicates that differences in the hydrophobic or vibrational contributions to binding cannot account for the observation of equivalent ΔG but differing ΔH. The hydrophobic contribution to antigen binding is equivalent for ch4D5 and hu4D5-8 Fab and is consistent with burial of about 960 Å^2 of nonpolar surface area upon complex formation.

Identification of the forces involved in the high affinity and specificity of antibody–antigen interaction requires detailed structural and functional characterization. Thermodynamic studies of antibody–antigen interaction are essential in this endeavor because the information present in ΔH, ΔS, and ΔC_p can provide insight into the mechanism of binding. For example, the magnitude of ΔC_p is related to the contribution of the hydrophobic effect to binding (Kauzmann, 1959; Tanford, 1980; Livingstone et al., 1991). Improvements in calorimeter sensitivity (Langerman & Biltonen, 1979; Weisman et al., 1989), as well as the development of bacterial expression systems for producing antibody Fab (Better et al., 1988) and Fv (Skerra & Plückthum, 1988) fragments, greatly facilitate thermodynamic studies of antibody–antigen interaction. The results of this approach should have an impact on the engineering of antibodies. For example, murine antibodies intended for human clinical use must be "humanized" (Riechmann et al., 1988) in order to reduce immunogenicity. In this procedure, the framework regions (Kabat et al., 1987) of the murine variable domains are replaced with human sequence. The sequences of the six hypervariable or CDR[1] loops, which provide the majority of the antigen contact residues (Davies & Metzger, 1983), are not altered. Since some framework residues may contact antigen or influence CDR conformation, successful humanization requires an understanding of structure–function relationships in antibody–antigen combining sites.

The murine monoclonal antibody 4D5 (mu4D5 MAb), raised against the extracellular domain of human epidermal growth factor receptor-2, shows promise for the treatment of certain breast and ovarian cancers which overexpress p185^{HER2}(Slamon et al., 1989; Shepard et al., 1991). mu4D5 MAb inhibits the proliferation of human breast tumor cells (SK-BR-3) in vitro (Hudziak et al., 1989). mu4D5 MAb was previously humanized by using molecular modeling to guide the replacement of murine framework residues with human consensus sequence (Carter et al., 1992a). Humanized 4D5 variants were constructed that differed in having murine or human residues at five framework positions that appeared

* Address correspondence to this author.
‡ Department of Protein Engineering.
§ Department of Cell Culture and Fermentation Research.
∥ Department of Protein Chemistry.
⊥ Department of Process Sciences.

[1] Abbreviations: p185^{HER2}, human epidermal growth factor receptor 2 (also called *c-erbB-2*); p185$^{HER2\text{-}ECD}$, extracellular domain of p185^{HER2}; RIA, radioimmunoassay; CDR, complementarity determining region; FR, framework region; hu, humanized; ch, chimeric; mu, murine; PBS, phosphate-buffered saline.

0006-2960/92/0431-5434$03.00/0

Table I: Sequence Differences between 4D5 Fab Variants[a]

	V_H residue					V_L residue				
Fab	71 FR3	73 FR3	78 FR3	93 FR3	102 CDR3	55 CDR2	66 FR3	expected mass	observed mass[b]	T_m[c] °C
ch4D5	A	T	A	S	Y	Y	R	48 120	48 121 ± 5	72.4
hu4D5-1[d]	R	D	L	A	V	E	G	47 666	47 666 ± 3	ND
hu4D5-2	A	D	L	A	V	E	G	47 581	47 583 ± 3	ND
hu4D5-3	A	T	A	S	V	E	G	47 541	47 528 ± 4	84.2
hu4D5-4	A	T	L	S	V	E	R	47 682	47 672 ± 4	79.6
hu4D5-5	A	T	A	S	V	E	R	47 640	47 641 ± 3	82.2
hu4D5-6	A	T	A	S	V	Y	R	47 674	47 662 ± 5	84.6
hu4D5-7	A	T	A	S	Y	E	R	47 704	47 693 ● 7	ND
hu4D5-8	A	T	A	S	Y	Y	R	47 738	47 738 ± 3	82.5

[a] This set of residues, in addition to CDR residues, appeared to be important for antigen binding on the basis of molecular modeling and functional analysis of variant MAbs (Carter et al., 1991a). Residues are numbered according to Kabat et al. (1987). In addition to the differences shown, ch4D5 differs from hu4D5 at 21 framework sites in V_L and 32 framework sites in V_H. [b] Molecular weights were determined by electrospray-ionization mass spectrometry as described by Bourell et al. (1992). [c] Melting temperature (T_m) at pH 5 was determined by differential scanning calorimetry. ND = not determined. [d] Human consensus sequence.

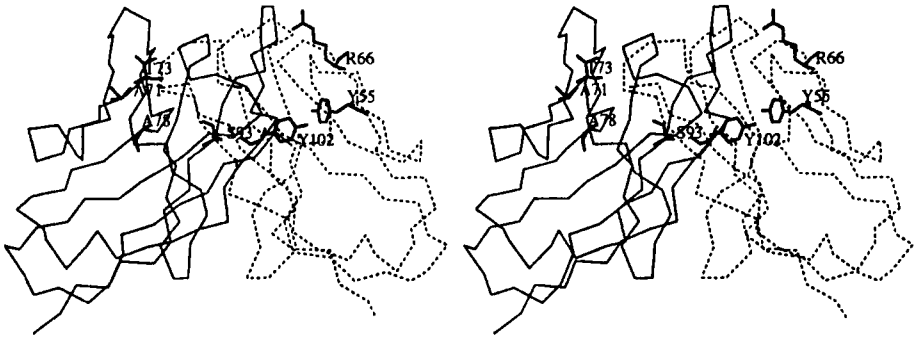

FIGURE 1: Structure of the Fv fragment of hu4D5-8 determined by X-ray crystallography to 2.2-Å resolution (C. Eigenbrot, unpublished results). α-Carbon trace of the heavy chain (solid line) and light chain (dotted line) is shown in a stereodiagram. Side chains of framework residues of murine origin are numbered and shown in thicker lines. The orientation of molecule is with CDR loops on top.

important for antigen binding either in determining CDR conformation or as antigen contact residues (Table I; Figure 1). In addition to these five framework residues, measurements of K_D values by using an ELISA method (Friguet et al., 1985) indicated that tyrosine residues at sites V_L-55 and V_H-102 were required in order to attain the antigen affinity measured for the murine antibody. These two positions are considered to be CDR residues by sequence hypervariability (Kabat et al., 1987) but not by structural criteria (Chothia & Lesk, 1987). Although hu4D5-8 MAb and mu4D5 MAb have comparable antigen affinity, hu4D5-8 MAb has decreased antiproliferative activity. In addition, the antiproliferative activities of the humanized variants are not strongly correlated with antigen affinity. For example, hu4D5-5 MAb binds antigen with 10-fold reduced affinity but has antiproliferative activity comparable to that of hu4D5-8 MAb.

We describe here results of biochemical and biophysical studies on chimeric and humanized 4D5 Fab fragments aimed at understanding the determinants of antigen binding and biological activity. (ch4D5 Fab has whole murine variable domains fused to human constant domains). Fab fragments, owing to their smaller size, monovalency, and greater solubility, are more amenable to biophysical studies than intact antibodies. Production of Fab fragment was facilitated by high-level (0.5–2 g/L) expression in *Escherichia coli* (Carter et al., 1992b) and tight binding of hu4D5 Fab to *Staphylococcus aureus* protein A. ΔH values for antigen binding were determined by using isothermal calorimetry and an RIA method was developed for measuring binding constants. Framework residue contributions to antigen binding were assessed by determining these parameters for the variants shown in Table I. The role of the hydrophobic effect in antigen binding was addressed by determining ΔC_p for ch4D5 and hu4D5-8 Fab from the temperature dependence of ΔH. ΔC_p values were also determined for humanized variants differing from hu4D5-8 at sites V_L-55 and V_H-102. As shown in Figure 1, the V_L-Y55 and V_H-Y102 side chains are close to the CDR loops and could directly participate in antigen binding. A tyrosine side chain might contribute to binding through the hydrophobic effect, or via hydrogen bonding, and ΔC_p values should be useful in discriminating between these mechanisms. Finally, the antiproliferative activity of 4D5 Fab fragments on SK-BR-3 cells was determined.

Experimental Procedures

Materials. DEAE-Sepharose-FF, S-Sepharose-FF, and streptococcal protein G–Sepharose were from Pharmacia, Inc. ProSep-A HC, staphylococcal protein A coupled to controlled-pore glass, was from BioProcessing, Ltd. Toyopearl phenyl 650M hydrophobic interaction chromatography medium was from TosoHaas. Membranes for tangential flow filtration were from Filtron, Inc. Goat anti-human and anti-mouse IgG antisera were purchased from Fitzgerald, Inc.

Expression of Fab Fragments in E. coli. hu4D5 and ch4D5 Fab fragments were expressed by secretion from *E. coli* using derivatives of the plasmid pAK19 (Carter et al., 1992b). These derivatives lack the hinge cysteines which form the inter-heavy chain disulfides in $F(ab')_2$ fragments. hu4D5 variants differing by a few variable domain residues were subcloned from a mammalian expression vector (Carter et al., 1992a) into pAK19. *E. coli* cells transformed with these plasmids were grown in a 10-L fermentor as described previously (Carter et al., 1992b) except that the agitation rate was increased to 1000 rpm. The majority of the expressed Fab fragment was found in the supernatant fraction obtained after removal of the cells by centifugation. Titers of hu4D5 Fab fragments were rou-

Table II: Antigen Binding Thermodynamics for 4D5 Fab Fragments[a]

4D5 Fab[b]	K_D (pM)	$\Delta G°$ (kcal mol^{-1})	ΔH (kcal mol^{-1})	$\Delta S°$ (cal mol^{-1} K^{-1})	ΔC_p[c] (cal mol^{-1} K^{-1})
ch4D5	150 ± 90	−13.5 ± 0.4	−17.2 ± 1.5	−12	−400 ± 40
hu4D5-5 (V_H-V102, V_L-E55)	430 ± 120	−12.8 ± 0.2	−10.0 ± 0.6	+9	−320 ± 20
hu4D5-6 (V_H-V102, V_L-Y55)	159	−13.4	−11.4	+7	−400 ± 30
hu4D5-8 (V_H-Y102, V_L-Y55)	90 ± 30	−13.7 ± 0.1	−12.9 ± 0.4	+3	−370 ± 30

[a] Standard state is unit molarity. $\Delta G°$ was calculated using the standard equation, $\Delta G° = -RT \ln K$, where $K = 1/K_D$, $T = 298.55$ K, $R = 1.99$ cal mol^{-1} K^{-1}. ND = not determined. K_D and ΔH values shown with standard deviations are the mean of three or more determinations; other values are from single measurements. [b] Residues at sites V_L-55 and V_H-102 are shown in parentheses for humanized variants. [c] ΔC_p was determined from the slope of the temperature dependence of ΔH between 25 and 45 °C. In this range, ΔH displays a linear dependence on temperature suggesting that ΔC_p is independent of temperature.

tinely 0.5–2.0 g/L as judged by antigen binding ELISA (Carter et al., 1992b). ch4D5 Fab was poorly expressed at 37 °C (5–20 mg/L), but the expression level could be increased 10-fold by fermentation at 30 °C.

Purification of Fab Fragments from E. coli Supernatants. Fermentation supernatants (ca. 8 L) were microfiltered by using a tangential flow filtration (TFF) instrument equipped with a 2 ft^2, 0.16-μm membrane. The clarified supernatant was then concentrated 50-fold by ultrafiltration using a cellulose membrane having a molecular weight cutoff of 30000. This solution was diafiltered with 2 × 10 volumes of PBS and then filtered over DEAE-Sepharose-FF (ca. 200 mL) on a sintered glass funnel. hu4D5 Fab in the flow-through fraction was then subjected to affinity chromatography on a 5 × 10.5 cm column (200 mL) of ProSep-A. The column was washed with PBS, and then Fab was eluted with 0.1 M glycine, pH 3.0. Lower molecular weight contaminants were removed by hydrophobic interaction chromatography on a 5 × 7 cm column of Toyopearl phenyl 650M after the pool was adjusted to pH 4, 0.5 M ammonium sulfate. Fab eluted in the flow-through fraction. For ch4D5 Fab, which does not bind to protein A, the pool after passage over DEAE-Sepharose-FF was diafiltered against 10 mM MES, pH 5.5, and chromatographed on a 2.5 × 21 cm column of S-Sepharose-FF equilibrated with 10 mM MES, pH 5.5. Protein was eluted with a linear gradient of 0–0.5 M NaCl. Fractions containing Fab were pooled and subjected to affinity chromatography on a 2.5 × 5 cm column of protein G–Sepharose-FF equilibrated with 10 mM MES, pH 5.5. ch4D5 Fab was eluted with 0.1 M glycine, pH 3. Concentrations of both ch4D5 and hu4D5 Fab were determined by A_{280} measurements using an ϵ_{280} of 67 mM^{-1} cm^{-1} determined by quantitative amino acid analysis.

Purification of p185$^{HER-ECD}$ and mu4D5 MAb. p185$^{HER2-ECD}$ was purified from CHO cell harvest fluid concentrate as previously described (Fendly et al., 1990a). An ϵ_{280} of 76 mM^{-1} cm^{-1}, determined by quantitative amino acid analysis, was used to determine concentrations of solutions of purified p185$^{HER2-ECD}$. mu4D5 MAb was purified by using affinity chromatography on protein A–Sepharose as described by Fendly et al. (1990b).

Circular Dichroic Spectroscopy. Circular dichroic spectra were recorded on an Aviv/Cary spectropolarimeter. A series of 10 spectra were collected and averaged for each sample using a time constant of 1.0 s, a spectral bandwidth of 1.0 nm, and a wavelength interval of 0.5 nm. Quartz, cylindrical cells having a path length of 1 cm, for near-UV CD, or 0.05 cm, for far-UV CD, were used. Fab solutions were prepared for near-UV, CD measurements by dialysis versus 20 mM sodium phosphate, pH 7.5, 100 mM sodium chloride, and diluted to give an A_{280} of 1.0 in a 1-cm-path-length cell. These solutions were diluted 5-fold with distilled water for far-UV–CD measurements.

Differential Scanning Calorimetry. Thermal denaturation experiments were performed on a Microcal, Inc. (Northampton, MA) MC-2 differential scanning calorimeter. Fab solutions were prepared by extensive dialysis at ambient temperature versus 50 mM sodium acetate, pH 5. These solutions were adjusted to 2 mg/mL Fab and heated to 95 °C in the calorimeter using a heating rate of 1 °C/min. The observed melting profiles were baseline corrected and normalized using the software supplied by the manufacturer. Melting temperature (T_m) was not dependent on protein concentration in the range of 1–5 mg/mL but it did display a 2 °C decrease upon changing the heating rate to 0.2 °C/min.

Binding Constant Determination by RIA. p185$^{HER2-ECD}$ was labeled with ^{125}I using the sequential chloramine-T method (DeLarco et al., 1981) yielding a tracer having a specific activity of 14 μCi/μg. A series of 200-μL solutions containing 50 pM 4D5 Fab, 50 pM ^{125}I-labeled p185$^{HER2-ECD}$, and a varied amount of unlabeled antigen were prepared and incubated overnight at ambient temperature. Bound antigen was precipitated by addition of 100 μL goat anti-human IgG antisera (hu- and ch4D5 Fab) or goat anti-mouse IgG antisera (mu4D5 MAb). The complex formed with Fab required addition of 1 mL of 6% poly(ethylene glycol)-8000 for efficient precipitation. The amount of bound material was determined by γ counting of the immunoprecipitate using a LKB Instruments γ counter operating at 70% counting efficiency. A modified version of the program LIGAND (Munson & Rodbard, 1980) was used to determine the binding constant from these data. Similar dissociation constants were obtained whether the amount of total p185$^{HER2-ECD}$ was varied by adding increasing amounts of labeled, or unlabeled material, indicating that iodination of the receptor does not impair the antibody binding site.

RIA measurements of the binding of mu4D5 MAb to p185$^{HER2-ECD}$ reveal a K_D of 60 ± 20 pM as compared with a K_D of 300 pM determined by using an ELISA method (Carter et al., 1992a). Both methods measure binding of soluble antigen to soluble antibody and thus are free of avidity effects. The discrepancy in K_D values is probably related to the greater sensitivity afforded by radiochemical detection. Thus, lower 4D5 concentrations can be used in the RIA method allowing a more accurate determination of K_D.

Determination of the Enthalpy of Binding. The enthalpy change (ΔH) associated with binding of 4D5 variants to p185$^{HER2-ECD}$ was determined by using isothermal calorimetry on a Microcal, Inc. OMEGA titration calorimeter. Measurements were performed using solutions that had been extensively dialyzed versus 20 mM sodium phosphate, pH 7.5, 100 mM sodium chloride. Antigen and antibody were dialyzed in the same vessel in order to minimize mixing heat effects due to differences in solution composition. A titration protocol in which a 2-fold excess of antibody was obtained by making six equal volume injections was usually employed. The p185$^{HER2-ECD}$ concentration was 7–10 μM. This concentration of antigen was required for precise enthalpy measurements but precludes calorimetric measurement of K_D (Wiseman et

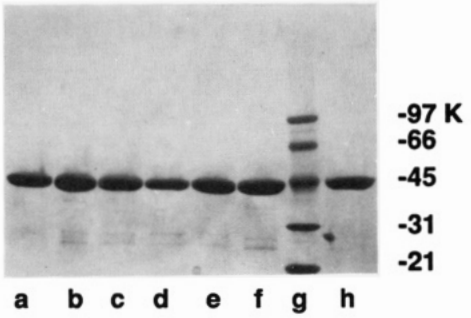

FIGURE 2: SDS–PAGE of purified Fab fragments: (a) ch4D5; (b) hu4D5-5; (c) hu4D5-4; (d) hu4D5-3; (e) hu4D5-8; (f) hu4D5-2; (g) molecular weight standard; (h) hu4D5-1.

al., 1989) given the magnitude of the binding constants (Table II). Heats of reaction were determined using the software supplied by the manufacturer, heats of Fab dilution were subtracted, and the corrected heats were summed and divided by the moles of the receptor titrated to obtain ΔH.

RESULTS

Production of Fab Fragments. hu4D5 Fab fragments were readily purified from *E. coli* supernatants owing to the high expression levels (0.5–2 g/L) and tight binding to immobilized *S. aureus* protein A. A total of 0.5–1.5 g of hu4D5 Fab could be rapidly purified from 8 L of fermentation supernatant. The yield of the protocol was limited by the capacity (ca. 6 mg of hu4D5 Fab/mL of ProSep-A) of the protein A column. Although evidence for protein A binding to the Fab portion of IgG has been previously described (Inganäs et al., 1980), this is the first demonstration, to our knowledge, of the use of protein A in the purification of IgG Fab fragments. Since ch4D5 Fab does not bind protein A and also is expressed at a lower level, this variant was purified using a cation-exchange step followed by affinity chromatography on streptococcal protein G–Sepharose.

As shown in Figure 2, both ch4D5 and hu4D5 Fab fragments purified from *E. coli* are fairly homogeneous. Electrospray-ionization mass spectrometry indicates that ch4D5, hu4D5-1, hu4D5-2, hu4D5-5, and hu4D5-8 Fab have masses that agree closely with those expected from their sequence (Table I). Reduction of these Fab fragments prior to mass spectrometry yielded molecular ions consistent with the masses expected for the component light and heavy chains (data not shown). All of the other Fab fragments have observed masses differing from the expected molecular weight by 15 mass units or less. For these variants, the discrepancy between the observed and expected mass was smaller for the reduced fragments (data not shown). Other sequences present as contaminants would most likely not be detected by mass spectrometry unless present at levels of 10% or more of total protein. These data clearly show that the Fab fragments purified from *E. coli* supernatants have an interchain disulfide bond and are not proteolytically clipped or otherwise modified.

Conformation and Stability of E. coli Produced 4D5 Fab Fragments. ch4D5 Fab and all of the humanized Fab fragments gave far-UV–CD spectra consistent with that expected for an immunoglobulin fold (Doi & Jirgensons, 1970). CD spectra of ch4D5 and hu4D5-5 Fab are compared in Figure 3. ch4D5 and hu4D5 Fab spectra are superimposable between 240 and 210 nm but diverge at shorter wavelengths. Doi and Jirgensens (1970) have previously shown that the CD band at 202 nm shows greater variation between IgG samples than the 217-nm peak. The 202-nm peak also changes sign upon acid denaturation of IgG Fab fragments whereas the 217-nm

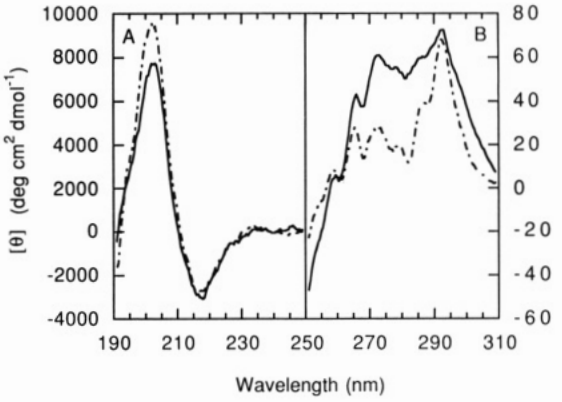

FIGURE 3: Circular dichroic spectra of recombinant Fab fragments in the far-UV (A) and near-UV (B) regions. The spectrum of ch4D5 Fab is shown as the solid line, whereas the hu4D5-5 spectrum is shown as the dashed line.

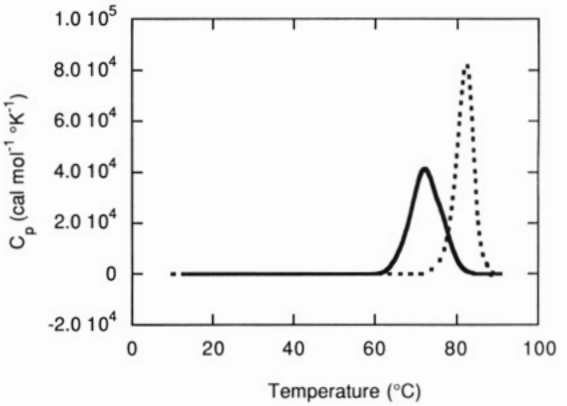

FIGURE 4: Thermal denaturation of 4D5 Fab fragments. The excess heat capacity profiles observed upon heating 2 mg/mL solutions of hu4D5-5 (dashed line) or ch4D5 Fab (solid line) containing 50 mM sodium acetate, pH 5, are shown.

peak is only modestly perturbed by this treatment. We conclude that CD measurements indicate 4D5 Fab fragments purified from *E. coli* supernatants are properly folded. The variation in the 202-nm peak, however, may indicate a subtle difference in conformation between chimeric and humanized 4D5 Fab fragments.

In the near-ultraviolet region, where CD arises primarily from asymmetry in the environment of aromatic side chains, the CD spectra of hu4D5 and ch4D5 Fab are not superimposable. No significant differences in near UV–CD are observed for a comparison of hu4D5 variants, although some of these differ in tyrosine composition (Table I). This observation suggests that the differences in near-UV–CD spectra between ch4D5 and hu4D5 Fab result from framework residue changes that have an impact on the environment of the aromatic chromophores.

hu4D5-5 Fab displays greater stability toward thermal denaturation than ch4D5 Fab as shown in Figure 4. Thermal denaturation of both proteins was not reversible as judged by cooling and reheating the sample. Aggregation may account for the poor reversibility as both Fab solutions were turbid after the second heating. Neither thermal transition could be described by a two-state process as the $\Delta H_{cal}/\Delta H_{VH}$ ratios were 3.7 and 2.3 for ch4D5 and hu4D5–5 Fab, respectively. Since ch4D5 and hu4D5-5 Fab have identical constant domains, the altered stability must arise from the framework changes in the variable domains. These changes may also alter V_L/V_H cooperativity as indicated by the decrease in $\Delta H_{cal}/\Delta H_{VH}$. As summarized in Table I, changes in variable domain residues

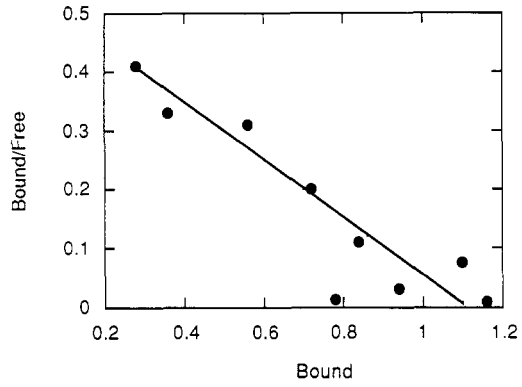

FIGURE 5: Scatchard plot of p185$^{HER2-ECD}$ binding to ch4D5 Fab measured by using an RIA at ambient temperature. The solid line is the result of analysis of these data using a modified version of the program LIGAND (Munson & Rodbard, 1980). These data are precisely described by a single binding site on the antigen having a K_D for Fab fragment of 103 pM. The intercept of the Scatchard plot on the x-axis indicates a stoichiometry of 1.07 mol of p185$^{HER2-ECD}$ bound/mol of Fab, as expected for a monovalent fragment.

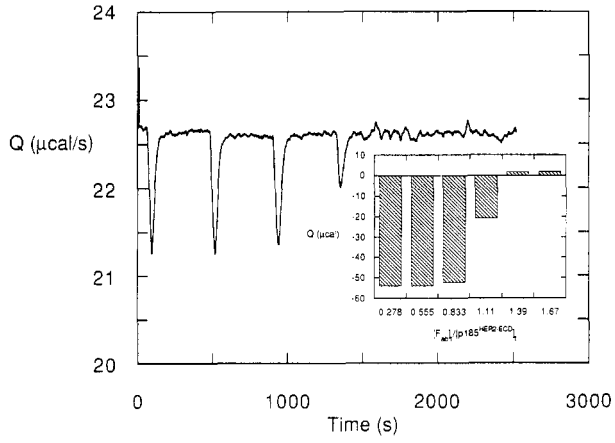

FIGURE 6: Calorimetric measurement of ch4D5 Fab binding to p185$^{HER2-ECD}$. A solution of p185$^{HER2-ECD}$ (8.5 μM) was titrated by injection of six aliquots (12 μL) of a solution of ch4D5 Fab (270 μM). The temperature was 25.4 ± 0.2 °C. The inset shows the heats of reaction, obtained by integration of the individual heat pulses, plotted as a function of the antibody to antigen ratio obtained at the end of the injection.

lead to small changes in thermal stability of hu4D5 Fab.

Thermodynamics of 4D5 Fab Binding to p185$^{HER2-ECD}$. Representative data for K_D determination by RIA and ΔH determination by isothermal calorimetry are shown in Figures 5 and 6, respectively. Scatchard analysis of the RIA data indicates a single class of binding sites and a stoichiometry of 1 mol of p185$^{HER2-ECD}$ bound/mol of Fab. As shown in Figure 6, large and negative heats of reaction are observed for substoichiometric additions of Fab to p185$^{HER2-ECD}$. These heat effects saturate upon addition of a stoichiometric amount of Fab. Small, positive heats are observed for further additions and are equivalent to heats of dilution measured in separate experiments by injection of Fab into a solution of buffer. Both RIA and calorimetry gave a precise measure of antigen binding with the variation of K_D being less than 2-fold and the standard error in ΔH measurements <10%. The highest affinity 4D5 Fab variants bind antigen with a K_D similar to that determined for mu4D5 MAb (K_D = 60 ± 20 pM).

$\Delta G°$ and ΔH values were determined for all of the 4D5 Fab variants shown in Table I. In addition, ΔC_p values were determined for ch4D5 and the hu4D5 variants that differ by substitutions at sites V_H–102 and V_L–55. (Thermodynamic parameters for these variants are shown in Table II.) Effects of amino acid substitutions on antigen binding are examined by calculating changes in $\Delta G°$, ΔH, and $\Delta S°$ using hu4D5–5 Fab as the reference molecule since it differs from several of the humanized variants by only single amino acid changes (Table III).

Table III: Effect of hu4D5 Variable Domain Substitutions on the Thermodynamics of Antigen Binding[a]

4D5 Fab	residue changes[b]	$\Delta\Delta G°$ (kcal mol^{-1})	$\Delta\Delta H$ (kcal mol^{-1})	$\Delta\Delta S°$ (cal mol^{-1} K^{-1})
hu4D5-1	V_H-A71R, T73D, A78L, S93A V_L-R66G	2.4	1.5	−3
hu4D5-2	V_H-T73D, A78L, S93A V_L-R66G	1.2	−0.4	−5
hu4D5-3	V_L-R66G	0.6	1.4	3
hu4D5-4	V_H-A78L	0	−1.5	−5
hu4D5-6	V_L-E55Y	−0.6	−1.4	−2
hu4D5-7	V_H-V102Y	0	0.1	1
hu4D5-8	V_H-V102Y V_L-E55Y	−0.9	−2.9	−6

[a] $\Delta\Delta J$ was calculated by subtracting the ΔJ value for hu4D5-5 from that measured for the variant. J = G, H, or S. [b] Amino acid replacements in going from hu4D5-5 to specified variant.

Comparison of ch4D5 and hu4D5-8 Fab Antigen Binding Thermodynamics. ch4D5 and hu4D5-8 Fab bind to p185$^{HER2-ECD}$ with comparable $\Delta G°$ values but significantly different enthalpy changes (Table II). As a consequence, the $\Delta S°$ terms have opposite signs. The heat capacity change associated with antigen binding is comparable for ch4D5 and hu4D5–8 Fab.

Role of V_L-Y55 and V_H-Y102 in Antigen Binding. Replacement of both residues (V_L-Y55E; V_H-Y102V) yields a variant (hu4D5-5 Fab) which binds to p185$^{HER2-ECD}$ with an affinity 4.8-fold lower (Table II) than that measured for hu4D5-8 Fab. Decreased affinity results from a less favorable ΔH that is partially offset by a more favorable ΔS. These changes also have a significant impact on ΔC_p. The single mutation V_L-E55Y (compare hu4D5-5 with hu4D5-6) results in a more favorable interaction with p185$^{HER2-ECD}$, as indicated by changes in both ΔG and ΔH, that is opposed by a less favorable ΔS. This single substitution restores ΔC_p to the value measured for binding of hu4D5-8 Fab. In contrast, the substitution V_H-V102Y has no effect upon binding when it is introduced as a single mutation (Table III).

Effect of Framework Residue Substitutions on Antigen Binding Thermodynamics. As previously reported for full-length hu4D5 variants produced in a mammalian expression system (Carter et al., 1991a), simple "grafting" of the 4D5 CDR residues onto a human consensus sequence results in a molecule with reduced affinity. This variant, hu4D5-1 Fab, binds to p185$^{HER2-ECD}$ with a K_D 60-fold larger than that measured for hu4D5-5 Fab. The decrease in affinity results from both a less favorable ΔH and a less favorable ΔS (Table III). The substitution V_L-R66G (hu4D5-5 → hu4D5-3) results in a 2.6-fold loss in affinity composed of a less favorable ΔH that is partially compensated by a more favorable ΔS. The substitution V_H-A78L (hu4D5-5 → hu4D5-4) leads to a more favorable enthalpy change in binding which is completely negated by a less favorable ΔS.

Biological Activity of Fab Fragments. The in vitro antiproliferative activity of 4D5 antibody toward the human breast tumor cell line SK-BR-3 was assayed as previously described (Carter et al., 1992a). Addition of increasing amounts of mu4D5 MAb to cultures of SK-BR-3 cells results in significant growth inhibition relative to the growth observed for a control culture having no added antibody (Figure 7). The maximal

Table IV: Contribution to Antigen Binding from Hydrophobic and Vibrational Effects[a]

4D5 Fab	ΔG_u[b]	ΔS_u	$\Delta C_{p(h)}$	ΔA_{np}[c] (Å^2)	$\Delta G_{u(h)}$[d]	$\Delta S_{u(h)}$	$\Delta C_{p(v)}$	$\Delta G_{u(v)}$	$\Delta H_{(v)}$	$\Delta S_{u(v)}$
ch4D5	−16	−4	−318	960	−24	83	−82	12.7	−13.0	−87
hu4D5-5	−15.2	17	−270	820	−20.5	70	−50	7.8	−7.9	−53
hu4D5-6	−15.8	15	−330	1000	−25.0	86	−70	10.9	−11.1	−71
hu4D5-8	−16.1	11	−305	920	−23.0	79	−65	10.1	−10.3	−68

[a] Values calculated using empirical method of Sturtevant (1977). Subscripts h and v denote hydrophobic and vibrational component, respectively. Units of ΔG and ΔH are kilocalories per mole; ΔC_p and ΔS units are calories per mole per Kelvin. [b] Unitary free energy (ΔG_u) and entropy (ΔS_u) changes are calculated assuming a standard state of unit mole fraction. These values were calculated from the values in Table II by adding the cratic entropy change, ΔS_c = +8 cal mol^{-1} K^{-1} (Kauzmann, 1959), to the observed ΔS values. [c] The amount of nonpolar surface area buried upon complex formation was calculated from $\Delta C_{p(h)}$ using a proportionality constant of 0.33 ± 0.09 cal mol^{-1} K^{-1} Å^{-2} (Livingstone et al., 1991) derived from hydrocarbon transfer experiments (Gill et al., 1976). An uncertainty of ±10% (±100 Å^2) in ΔA_{np} is estimated on the basis of the standard error in ΔC_p measurements and the variation in the proportionality constant. [d] $\Delta G_{u(h)}$ was calculated from ΔA_{np} using a proportionality constant of 25 cal mol^{-1} Å^{-2} (Chothia, 1974).

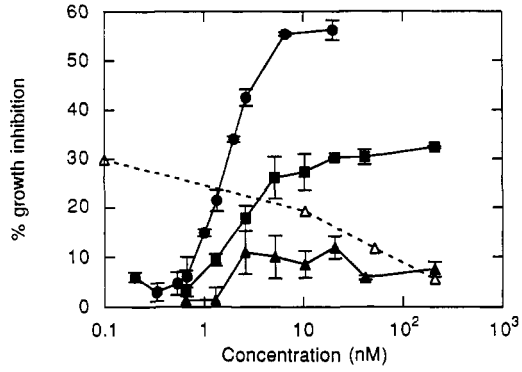

FIGURE 7: Antiproliferative effects of 4D5 variants on human breast tumor cell line SK-BR-3 assayed as previously described (Carter et al., 1992a). These data are reported as the percent of inhibition of growth relative to a control (0% inhibition) of no antibody addition. The concentration dependence of antiproliferative effects of mu4D5 MAb (●), ch4D5 Fab (■), and hu4D5-8 Fab (▲) is shown. The inhibition of the antiproliferative effect of 20 nM ch4D5 Fab by increasing amounts of hu4D5-8 Fab (△) is also shown.

growth inhibition is observed at about 10 nM mu4D5 MAb. Further increases in antibody concentration do not result in additional inhibition of growth. ch4D5 Fab has maximal antiproliferative activity equal to about half of that observed for the murine, bivalent antibody. If concentrations are expressed as the molarity of antigen binding sites, then the concentration of ch4D5 Fab required to produce half of the maximal effect is about the same as that observed for mu4D5 MAb. In contrast to these results, none of the hu4D5 Fab fragments display significant antiproliferative activity. Both ch4D5 Fab and hu4D5-8 Fab appear to bind to the same target on SK-BR-3 cells, as shown by the observation that increasing amounts of hu4D5-8 Fab inhibit the antiproliferative activity of ch4D5 Fab (Figure 7).

Discussion

Role of the Hydrophobic Effect in 4D5 Fab–Antigen Interaction. The contributions to antigen binding from the hydrophobic effect and intramolecular vibrations were analyzed using the empirical method of Sturtevant (1977). As shown in Table IV, the contribution to ΔC_p and ΔS_u calculated for the hydrophobic effect is large and approximately equivalent for ch4D5, hu4D5-6, and hu4D5-8 Fab. Binding of these variants to antigen appears to bury about 960 Å^2 of nonpolar surface area. If this interface is about 55% nonpolar, as is typical of protein–protein recognition sites (Janin & Chothia, 1990), then about 1750 Å^2 of the total surface area is buried in the complex. This contact area calculated from thermodynamic measurements agrees quite favorably with the mean value of 1600 ± 285 Å^2 of contact area calculated from X-ray crystallographic measurements of four antibody–antigen complexes (Janin & Chothia, 1990). The contribution from the hydrophobic effect for binding of hu4D5-5 Fab to antigen is considerably smaller suggesting that less nonpolar surface becomes buried in this complex.

Contributions to antigen binding from changes in vibrational modes are calculated to be large and to oppose binding. In contrast, a similar analysis for binding of a proteinaceous subtilisin inhibitor either to subtilisin BPN′ (Takahashi & Fukada, 1985) or to α-chymotrypsin (Fukada et al. 1985) indicated only minor contributions from changes in intramolecular vibrations. Antibody–antigen interaction, at least for the system described here, results in a greater loss of internal degrees of freedom than observed for protease–inhibitor interaction. This conclusion is consistent with the location of the antigen binding elements on flexible loops.

Comparison of ch4D5 and hu4D5-8 Fab Antigen Binding Thermodynamics. Differences in the magnitude of the hydrophobic effect cannot account for the difference in antigen binding ΔH between ch4D5 and hu4D5-8 Fab since the $\Delta C_{p(h)}$ terms are equivalent. Contributions to binding from changes in vibrational modes are more unfavorable for ch4D5 Fab and could account for almost 3 kcal mol^{-1} of the difference in ΔH between ch4D5 and hu4D5-8 Fab. However, the effect of these differences in vibrational modes on ΔG will be of similar magnitude but opposite sign. Thus, this simple analysis, which ignores contributions to ΔS_u from electrostatic interactions and conformational changes, indicates that differences in intramolecular vibrations cannot account solely for equivalent ΔG for ch4D5 and hu4D5-8 Fab and yet differing ΔH. Several alternative explanations may be considered. Subtle differences in electrostatic interactions or hydrogen bonding at the interface between CDR residues and antigen could contribute to these effects. For example, stronger salt-bridge formation with an arginine residue would tend to make ΔH more favorable, but restriction of the side chain would decrease ΔS. Given the size of the antigen, contacts with antibody framework residues that were not included in the humanized variants might account for the different properties. Preliminary results indicate that the ΔH for antigen binding to hu4D5-8 Fab can be made more exothermic by replacements in solvent accessible non-CDR loops (R. Kelley, unpublished results). Finally, a conformational change in the antigen–antibody complex that occurs for binding ch4D5 but not hu4D5-8 Fab could be involved. A change to a more ordered complex would be consistent with the unfavorable ΔS for ch4D5 Fab binding to antigen. A conformational change involving a displacement of V_H relative to V_L has been observed upon antigen binding to FvD1.3 (Bhat et al., 1990). Thermal denaturation experiments suggest that these domains unfold more independently in ch4D5 Fab than in hu4D5-5 Fab. Clearly, high-resolution structures of free and antigen-bound Fab are required to discriminate between these possibilities.

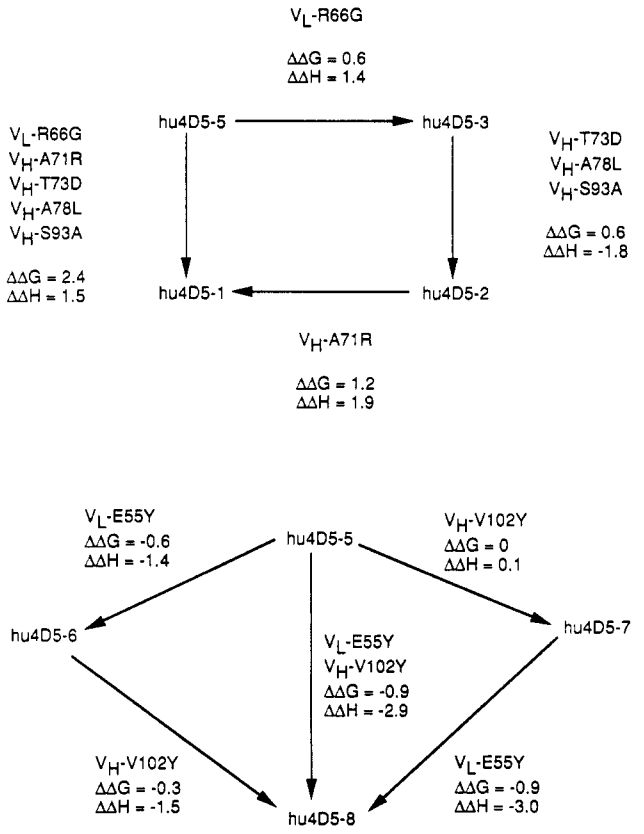

FIGURE 8: Schematic diagram illustrating additive effects of variable domain substitutions on antigen binding thermodynamics. $\Delta\Delta G$ and $\Delta\Delta H$ units are kilocalories per mole.

Additivity of Residue Replacements. As illustrated by the mutagenic scheme of Figure 8, the observed difference in antigen binding energetics between hu4D5-5 and hu4D5-1 Fab is exactly equal to the sum of the component changes. Additivity in $\Delta\Delta G$ values for multiple mutations is usually observed for residues that are not close in the structure [reviewed by Wells (1990)], as is the case for this set of framework residues (Figure 1). Additivity also applies to $\Delta\Delta H$ values between these sites. This relationship is particularly striking given the observation that the substitutions relating hu4D5-3 to hu4D5-2 result in a more favorable enthalpy change but decreased affinity. In contrast, V_L-Y55 and V_H-Y102, which are close in the structure, have nonadditive effects. For these sites, ΔH is also more sensitive to nonadditive relationships than ΔG.

Role of V_L-Y55 and V_H-Y102 in Antigen Binding. Although a structure of 4D5 bound to p185$^{HER2-ECD}$ has not been determined, a preliminary interpretation of the effects of residue replacements on antigen binding thermodynamics can be made on the basis of the structure of the free F_v fragment (Figure 1). The difference in $\Delta C_{p(h)}$ between hu4D5-5 and hu4D5-6 suggests that V_L-Y55 becomes buried in the interface with antigen and contributes to binding through the hydrophobic effect. This conclusion is consistent with the structure determined for hu4D5-8 F_v which shows the side chain of V_L-Y55 to be in van der Waals contact with the side chain of a residue from CDR-H3, V_H-F100. The V_L-Y55 side chain has 35 Å^2 of accessible nonpolar surface, as calculated from the Fv structure using the method of Lee and Richards (1971), a value considerably smaller than the difference of 180 Å^2 in ΔA_{np} calculated for hu4D5-5 and hu4D5-6 Fab (Table IV). Calculations of ΔA_{np} are subject to a standard error of about 10% (±100 Å^2) and include contributions from both antibody and antigen. In addition, since V_L-Y55 is in contact with V_H-F100, the replacement of V_L-Y55E may result in movement of V_H-F100 such that the contribution of ΔA_{np} from this residue is smaller. As shown in Table IV, the expected favorable contribution to ΔS_u from an increased hydrophobic interaction for hu4D5-6 F_{ab} is negated by an unfavorable $\Delta S_{u(v)}$. As a consequence, the improved binding of hu4D5-6 Fab is entirely an enthalpic effect, which is uncharacteristic of the hydrophobic effect (Kauzmann, 1959; Ross & Subramanian, 1981).

A comparison of the $\Delta C_{p(h)}$ values determined for hu4D5-6 and hu4D5-8 Fab suggests that V_H-Y102 does not contribute to binding through the hydrophobic effect. Thus, the improvement in binding would appear to result from increased hydrogen bonding with antigen. Hydrogen bonds between antibody tyrosine residues and antigen have been observed in the crystal structures determined for antibody–antigen complexes (Stanfield et al., 1990; Fischmann et al., 1991). The putative hydrogen bond(s) contributes −1.5 kcal mol^{-1} to ΔH and −4 cal mol^{-1} K^{-1} to ΔS. Interactions between V_L-Y55 and V_H-Y102 would be required to orient the side chain to make the hydrogen bond since the favorable contribution of V_H-Y102 requires the presence of V_L-Y55 (Table II; Figure 8).

Effect of Framework Residue Replacements on Antigen Binding. A comparison of hu4D5-3 and hu4D5-5 antigen binding data (Table III) shows that the contribution of V_L-R66 is similar to that expected for formation of a peptide hydrogen bond in water (Kauzmann 1959; $\Delta G = -0.4 \pm 0.1$ kcal mol^{-1}, $\Delta H = -1.4$ kcal mol^{-1}, $\Delta S = -3.3 \pm 1$ cal mol^{-1} K^{-1}). In the stucture of the Fv fragment the nonpolar part of the V_L-R66 side chain is not solvent accessible. A salt bridge is formed with V_L-D28 (CDR-L1) by using NH1 whereas NH2 of V_L-R66 is exposed and could make a hydrogen bond with antigen; however, a role for V_L-R66 in neutralizing the charge on V_L-D28 or determining the conformation of CDR-L1 cannot be excluded. Moreover, the results emphasize the importance of ΔC_p measurements in distinguishing hydrophobic from other effects since the dissimilar replacements V_L-R66G and V_L-E55Y have similar effects on ΔG and ΔH.

Tramontano et al. (1990) have previously proposed that framework residue V_H-71 is an important determinant of CDR-H2 conformation. This suggestion is confirmed for the 4D5 antibody as the V_H-A71R substitution (hu4D5-2 → hu4D5-1) results in an unfavorable (1.2 kcal mol^{-1}) change in the free energy of binding. This effect arises largely from a less favorable enthalpy change.

The substitution V_H-A78L has no effect on the ΔG of antigen binding but does result in a more favorable ΔH. V_H-A78 is a buried residue and was originally retained in the humanized molecule because modeling (Carter et al., 1992a) suggested that a Leu at this position could perturb the conformation of CDR-H1 through interactions with the side chains of V_H-F27 and V_H-I29. A preliminary comparison of the X-ray structure of hu4D5-4 Fab with that of hu4D5-8 Fv (C. Eigenbrot, unpublished results) shows that there is no movement of CDR-H1 associated with V_H-A78L but that the β-strand-containing residue 78 moves away from CDR-H1. This result suggests that the effect of V_H-A78L on ΔH is not due to changes in antibody–antigen contacts. Instead, the effects observed for V_H-A78L may involve changes in vibrational modes as described above; however, if the change in ΔH is due solely to vibrational effects, then the V_H-A78L mutation should have also resulted in a less favorable ΔG.

Antiproliferative Activity of ch4D5 Fab. Although p185^{HER2} appears to be a growth factor receptor, the mechanism of the 4D5 cytostatic effect remains unclear since the

binding sites for antibody and ligand have not been identified. We find that the monovalent Fab fragment of chimeric 4D5 retains antiproliferative activity on human tumor cells overexpressing p185^{HER2}. This result suggests that antibody-mediated receptor dimerization is not required for antiproliferative activity. Receptor dimerization may enhance this activity since bivalent mu4D5 MAb displays a 2-fold larger antiproliferative effect. Despite binding to p185$^{HER2-ECD}$ with an affinity equal to that measured for ch4D5 Fab, hu4D5-8 Fab does not have growth inhibitory properties. hu4D5-8 is active, however, if produced as bivalent F(ab')$_2$ fragment (Carter et al., 1992b). The difference in ΔH for binding of ch4D5 and hu4D5-8 Fab to p185$^{HER2-ECD}$ suggests that the antiproliferative activity of ch4D5 Fab has its origins in the details of binding to the extracellular domain. Thus, the possibilities suggested above for the differences in antigen binding thermodynamics may also explain the differences in antiproliferative activity. These results show that construction of a humanized antibody based on measurements of binding constants alone may not reproduce the desired biological properties of the murine antibody.

Acknowledgments

We are grateful to Greg Bennett and Drs. Beth Hutchins and Wai-Lee Wong for help with RIA development. We thank Dr. Greg Blank for supplying purified mu4D5 MAb. Dr. Robert VanReis is thanked for guidance in the use of tangential flow filtration. We acknowledge Monique Carver and Dr. Claire Kotts for the assay of antiproliferative activities.

References

Better, M., Chang, C. P., Robinson, R. R., & Horwitz, A. H. (1988) *Science 240*, 1041–1043.

Bhat, T. N., Bentley, G. A., Fischmann, T. O., Boulot, G., & Poljak, R. J. (1990) *Nature 347*, 483–485.

Bourell, J. H., Stults, J. T., Clauser, K., Carter, P., & Kelley, R. F. (1992) *Anal. Chem.* (submitted for publication).

Davies, D. R., & Metzger, H. (1983) *Annu. Rev. Immunol. 1*, 87–117.

Carter, P., Presta, L., Gorman, C. M., Ridgway, J. B. B., Henner, D., Wong, W.-L. T., Rowland, A. M., Kotts, C., Carver, M. E., & Shepard, H. M. (1992a) *Proc. Natl. Acad. Sci. U.S.A.* (in press).

Carter, P., Kelley, R. F., Rodrigues, M. L., Snedecor, B., Covarrubias, M., Velligan, M. D., Wong, W.-L. T., Rowland, A. M., Kotts, C. E., Carver, M. E., Yang, M., Bourell, J. H., Shepard, H. M., & Henner, D. (1992b) *Bio/Technology 10*, 163–167.

Chothia, C. (1974) *Nature 248*, 338–339.

Chothia, C., & Lesk, A. M. (1987) *J. Mol. Biol. 196*, 901–917.

DeLarco, J. E., Preston, Y. A., & Todaro, G. J. (1981) *J. Cell. Physiol. 109*, 143–152.

Doi, E., & Jirgensons, B. (1970) *Biochemistry 9*, 1066–1073.

Fendly, B. M., Kotts, C., Vetterlein, D., Lewis, G. D., Winget, M., Carver, M. E., Watson, S. R., Sarup, J., Saks, S., Ullrich, A., & Shepard, H. M. (1990a) *J. Biol. Response Modif. 9*, 449–455.

Fendly, B. M., Winget, M., Hudziak, R. M., Lipari, M. T., Napier, M. A., & Ullrich, A. (1990b) *Cancer Res. 50*, 1550–1558.

Fischmann, T. O., Bentley, G. A., Bhat, T. N., Boulot, G., Mariuzza, R. A., Phillips, S. E. V., Tello, D., & Polijak, R. J. (1991) *J. Biol. Chem. 266*, 12915–12920.

Friguet, B., Chaffotte, A. F., Djavadi-Ohaniance, L., & Goldberg, M. E. (1985) *J. Immunol. Methods 77*, 305–319.

Fukada, H., Takahashi, K., & Sturtevant, J. M. (1985) *Biochemistry 24*, 5109–5115.

Gill, S. J., Nichols, N. F., & Wadso, I. (1976) *J. Chem. Thermodyn. 8*, 445–452.

Hudziak, R. M., Lewis, G. D., Winget, M., Fendly, B. M., Shepard, H. M., & Ullrich, A. (1989) *Mol. Cell. Biol. 9*, 1165–1172.

Inganäs, M., Johansson, S. G. O., & Bennich, H. H. (1980) *Scand. J. Immunol. 12*, 23–31.

Janin, J., & Chothia, C. (1990) *J. Biol. Chem. 265*, 16027–16030.

Kabat, E. A., Wu, T. T., Reid-Miller, M., Perry, H. M., & Gottesman, K. S. (1987) *Sequences of proteins of immunological interest*, 4th ed., NIH, Washington, D.C.

Kauzmann, W. (1959) *Adv. Protein Chem. 14*, 1–63.

Langerman, N., & Biltonen, R. L. (1979) *Methods Enzymol. 61*, 261–286.

Lee, B., & Richards, F. M. (1971) *J. Mol. Biol. 55*, 379–400.

Livingstone, J. R., Spolar, R. S., & Record, M. T. (1991) *Biochemistry 30*, 4237–4244.

Munson, P. J., & Rodbard, D. (1980) *Anal. Biochem. 107*, 220–239.

Riechmann, L., Clark, M., Waldmann, H., & Winter, G. (1988) *Nature 332*, 323–329.

Ross, P. D., & Subramanian, S. (1981) *Biochemistry 20*, 3096–3102.

Shepard, H. M., Lewis, G. D., Sarup, J. C., Fendly, B. M., Maneval, D., Mordenti, J., Figari, I., Kotts, C. E., Palladino, M. A., Ullrich, A., & Slamon, D. (1991) *J. Clin. Immunol. 11*, 117–127.

Skerra, A., & Plückthun, A. (1988) *Science 240*, 1038–1041.

Slamon, D., Clark, G. M., Wong, S. G., Levin, W. J., Ullrich, A., & McGuire, W. L. (1987) *Science 235*, 177–181.

Slamon, D., Godolphin, W., Jones, L. A., Holt, J. A., Wong, S. G., Keith, D. E., Levin, W. J., Stuart, S. G., Udove, J., Ullrich, A., & Press, M. F. (1989) *Science 244*, 707–712.

Stanfield, R. L., Fieser, T. M., Lerner, R. A., & Wilson, I. A. (1990) *Science 248*, 712–719.

Sturtevant, J. M. (1977) *Proc. Natl. Acad. Sci. U.S.A. 74*, 2236–2240.

Takahashi, K., & Fukada, H. (1985) *Biochemistry 24*, 297–300.

Tanford, C. (1980) *The Hydrophobic Effect*, 2nd ed., Wiley-Interscience, New York.

Tramontano, A., Chothia, C., & Lesk, A. M. (1990) *J. Mol. Biol. 215*, 175–182.

Wells, J. A. (1990) *Biochemistry 29*, 8509–8517.

Wiseman, T., Williston, S., Brandts, J. F., & Lin, L.-N. (1989) *Anal. Biochem. 179*, 131–137.